Detection of very high energy gamma-ray emission from the gravitationally lensed blazar QSO B0218+357 with the MAGIC telescopes

ABSTRACT

Context. QSO B0218+357 is a gravitationally lensed blazar located at a redshift of 0.944. The gravitational lensing splits the emitted radiation into two components that are spatially indistinguishable by gamma-ray instruments, but separated by a 10–12 day delay. In July 2014, QSO B0218+357 experienced a violent flare observed by the *Fermi*-LAT and followed by the MAGIC telescopes.

Aims. The spectral energy distribution of QSO B0218+357 can give information on the energetics of $z \sim 1$ very high energy gamma-ray sources. Moreover the gamma-ray emission can also be used as a probe of the extragalactic background light at $z \sim 1$.

Methods. MAGIC performed observations of QSO B0218+357 during the expected arrival time of the delayed component of the emission. The MAGIC and *Fermi*-LAT observations were accompanied by quasi-simultaneous optical data from the KVA telescope and X-ray observations by *Swift*-XRT. We construct a multiwavelength spectral energy distribution of QSO B0218+357 and use it to model the source. The GeV and sub-TeV data obtained by *Fermi*-LAT and MAGIC are used to set constraints on the extragalactic background light.

Results. Very high energy gamma-ray emission was detected from the direction of QSO B0218+357 by the MAGIC telescopes during the expected time of arrival of the trailing component of the flare, making it the farthest very high energy gamma-ray source detected to date. The observed emission spans the energy range from 65 to 175 GeV. The combined MAGIC and *Fermi*-LAT spectral energy distribution of QSO B0218+357 is consistent with current extragalactic background light models. The broadband emission can be modeled in the framework of a two-zone external Compton scenario, where the GeV emission comes from an emission region in the jet, located outside the broad line region.

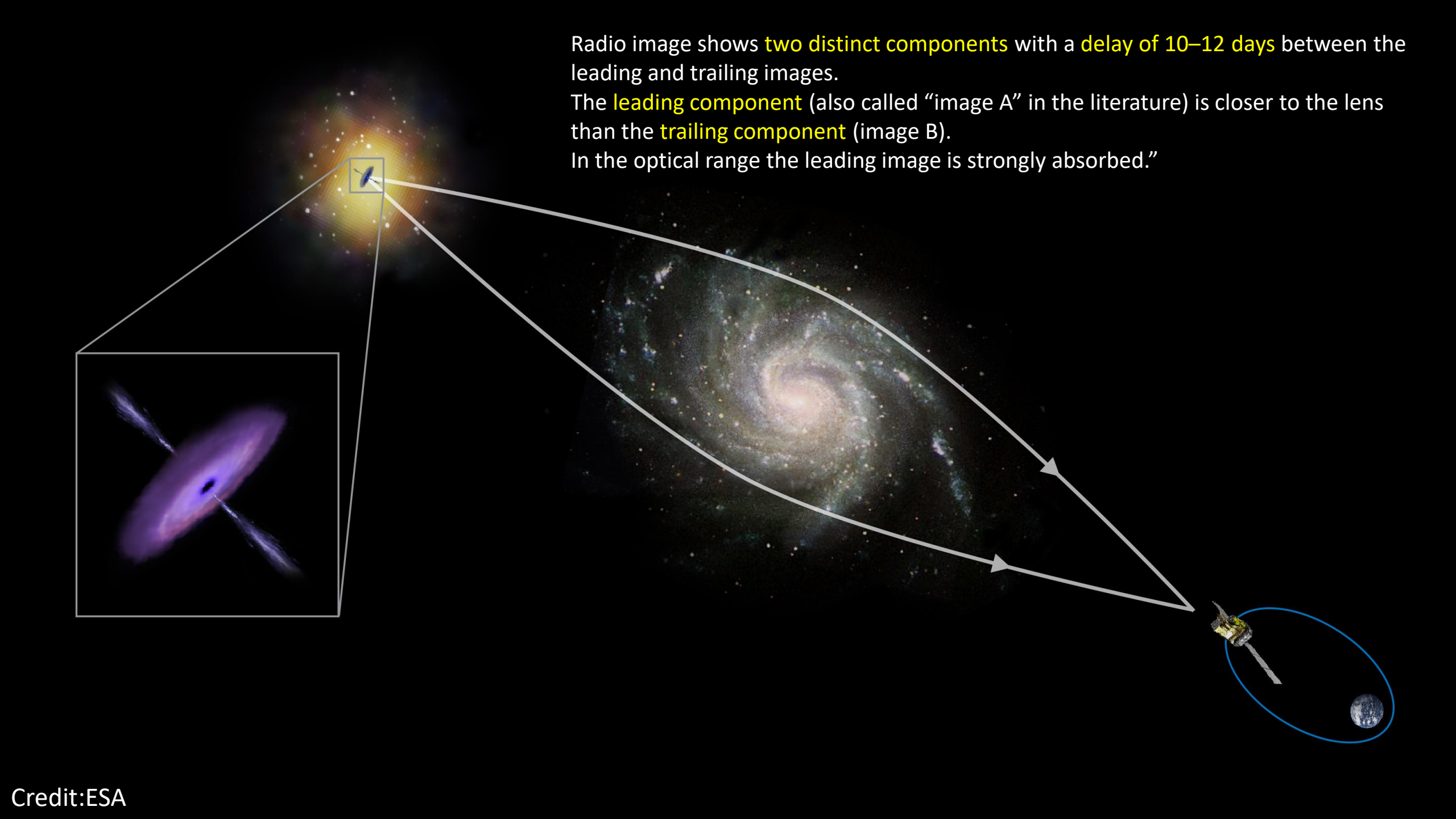
Radio image shows two distinct components with a delay of 10–12 days between the leading and trailing images.
The leading component (also called “image A” in the literature) is closer to the lens than the trailing component (image B).
In the optical range the leading image is strongly absorbed.”
Credit:ESA

LENSING GALAXY

- Magnification
- Microlensing
- Absorption
- Time Delay

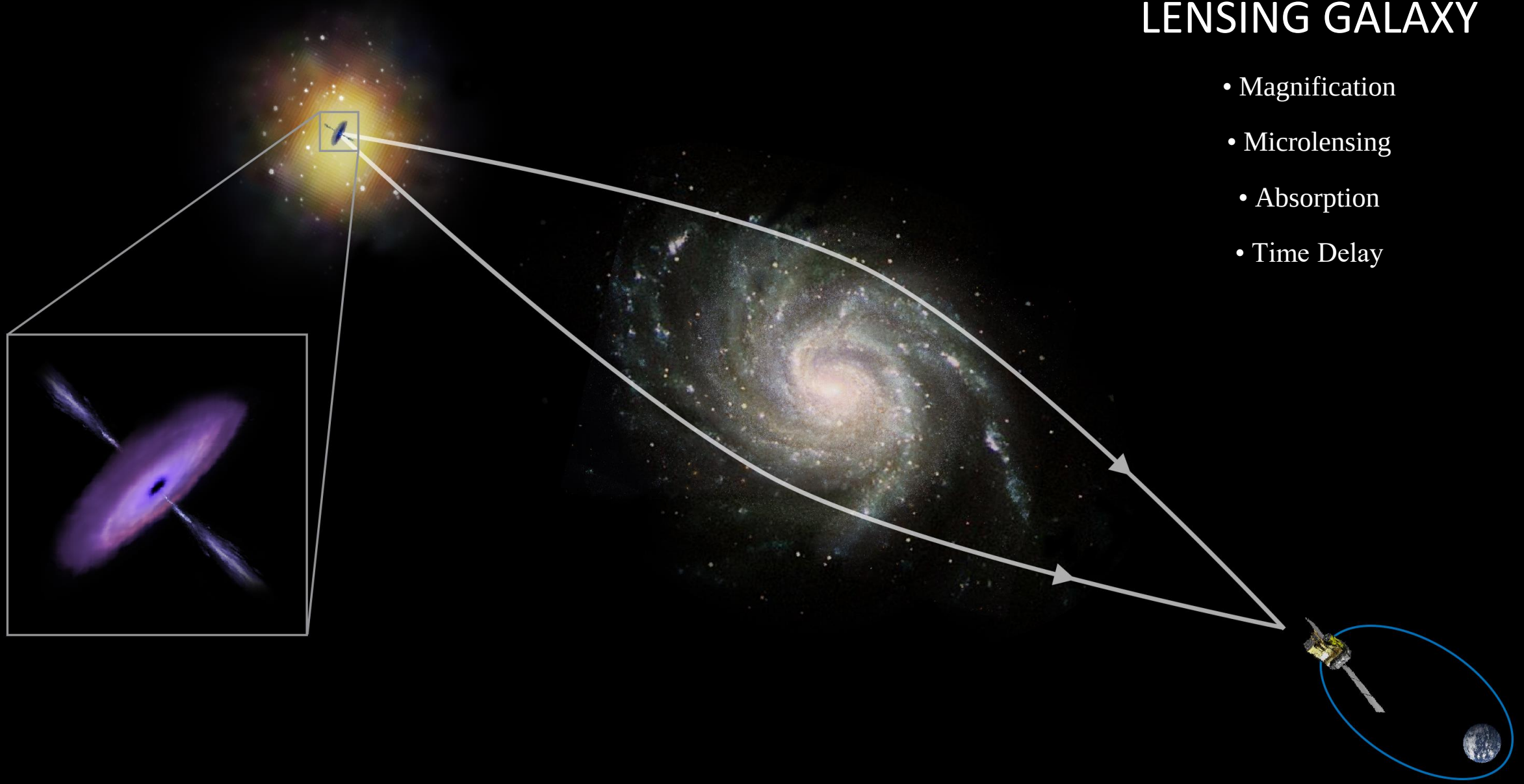

Credit:ESA

“The VHE (>100GeV) gamma-ray observations of QSO B0218+357 during the flaring state in July 2014 were performed with the MAGIC telescopes. The source was also monitored in GeV energies by *Fermi*-LAT, in X-ray by *Swift*-XRT and in optical by KVA.”

LIGHT CURVE

Fig. 2. Light curve of QSO B0218+357 during the flaring state in July/August 2014. *Top panel*: MAGIC (points) above 100 GeV and a Gaussian fit to the peak position (thick solid line). *Second panel from the top*: *Fermi*-LAT above 0.3 GeV with the average flux from the 3rd *Fermi* Catalog (Acero et al. 2015) marked with a dashed line. Notice that, during the days where the trailing emission was expected *Fermi*-LAT was in pointing mode allowing the significant detection of lower flux levels. *Third panel from the top*: *Swift*-XRT count rate in the 0.3–10 keV range. *Bottom panel*: KVA in *R* band (not corrected for the contribution of host/lens galaxies and the Galactic extinction). The two shaded regions are separated by 11.46 days.

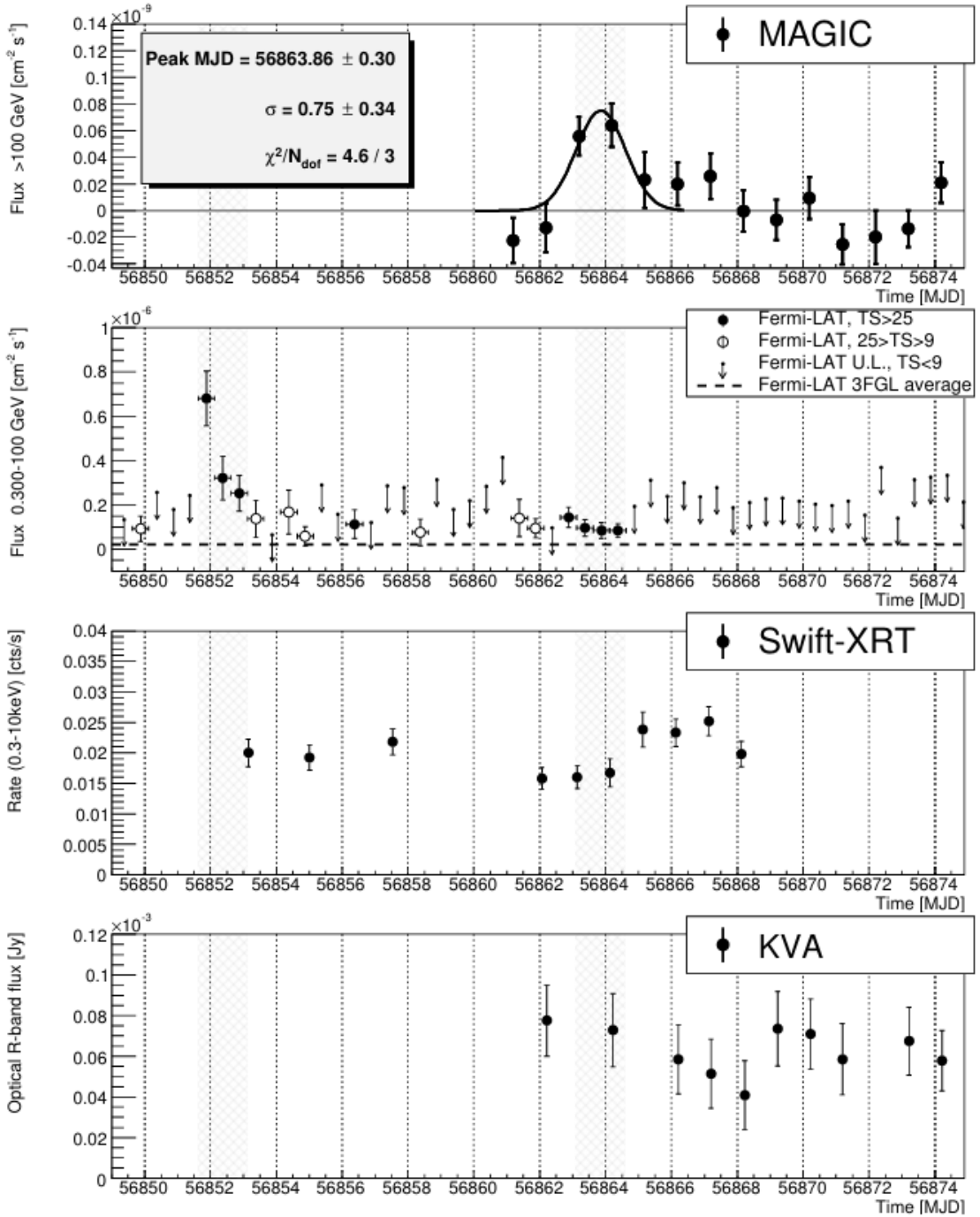

LIGHT CURVE

- not immediately follow the flare alert
- observations 10 days later -> delayed component
- fit with a Gaussian function.
- systematic error due to the 15% uncertainty in the energy scale.

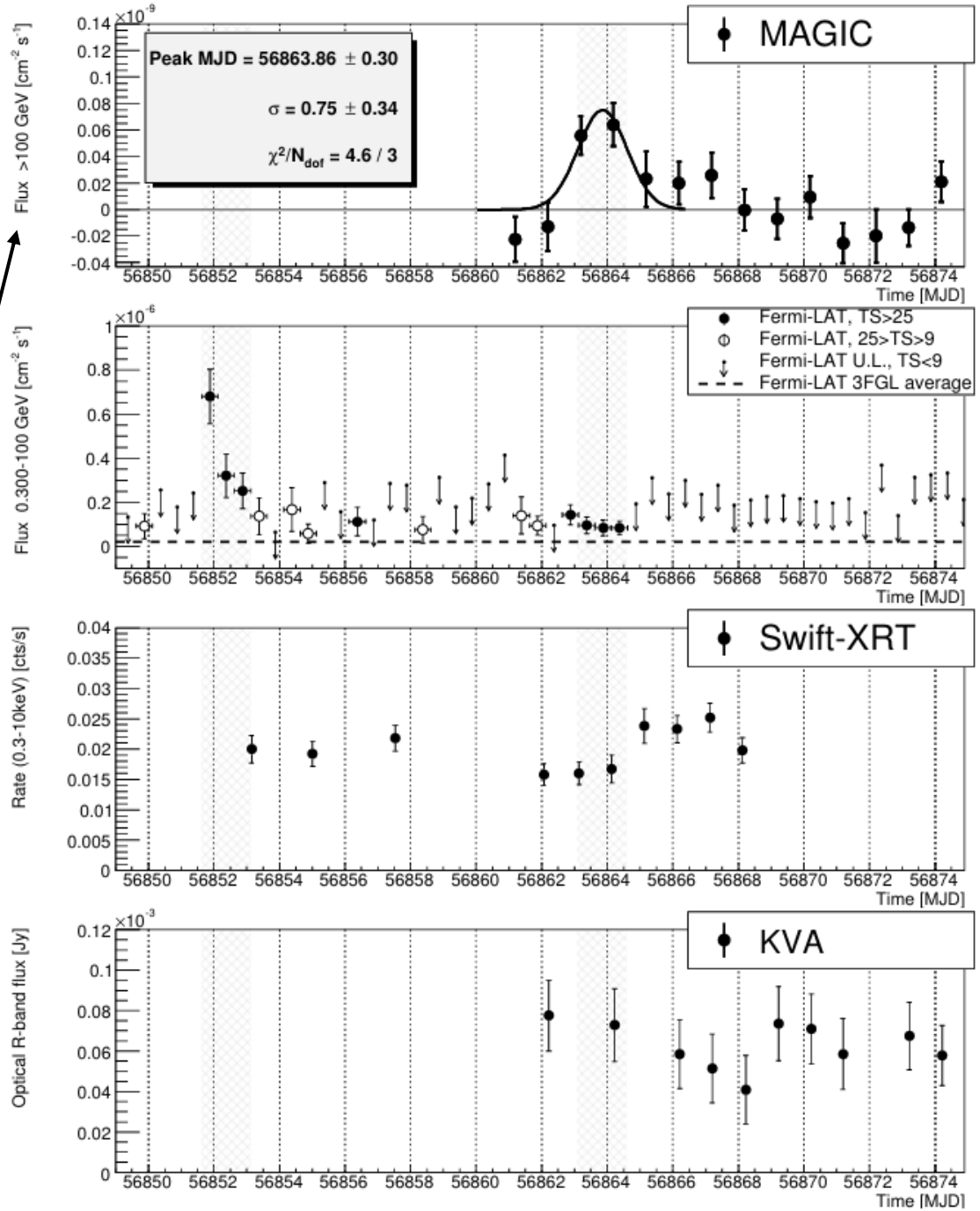

LIGHT CURVE

- energy range 0.1–300 GeV but **minimum energy 0.3 GeV** (the PSF of LAT at 0.1 GeV is about twice larger than that at 0.3 GeV)
- Significant GeV gamma-ray emission both during the leading flare and during the expected arrival time of the delayed emission (TS of 615 and 129 respectively)
- The spectrum contemporaneous to the MAGIC detection can be described by a power-law function

Test Statistic (TS)
Quantifies the probability of having a point gamma-ray source at the location specified

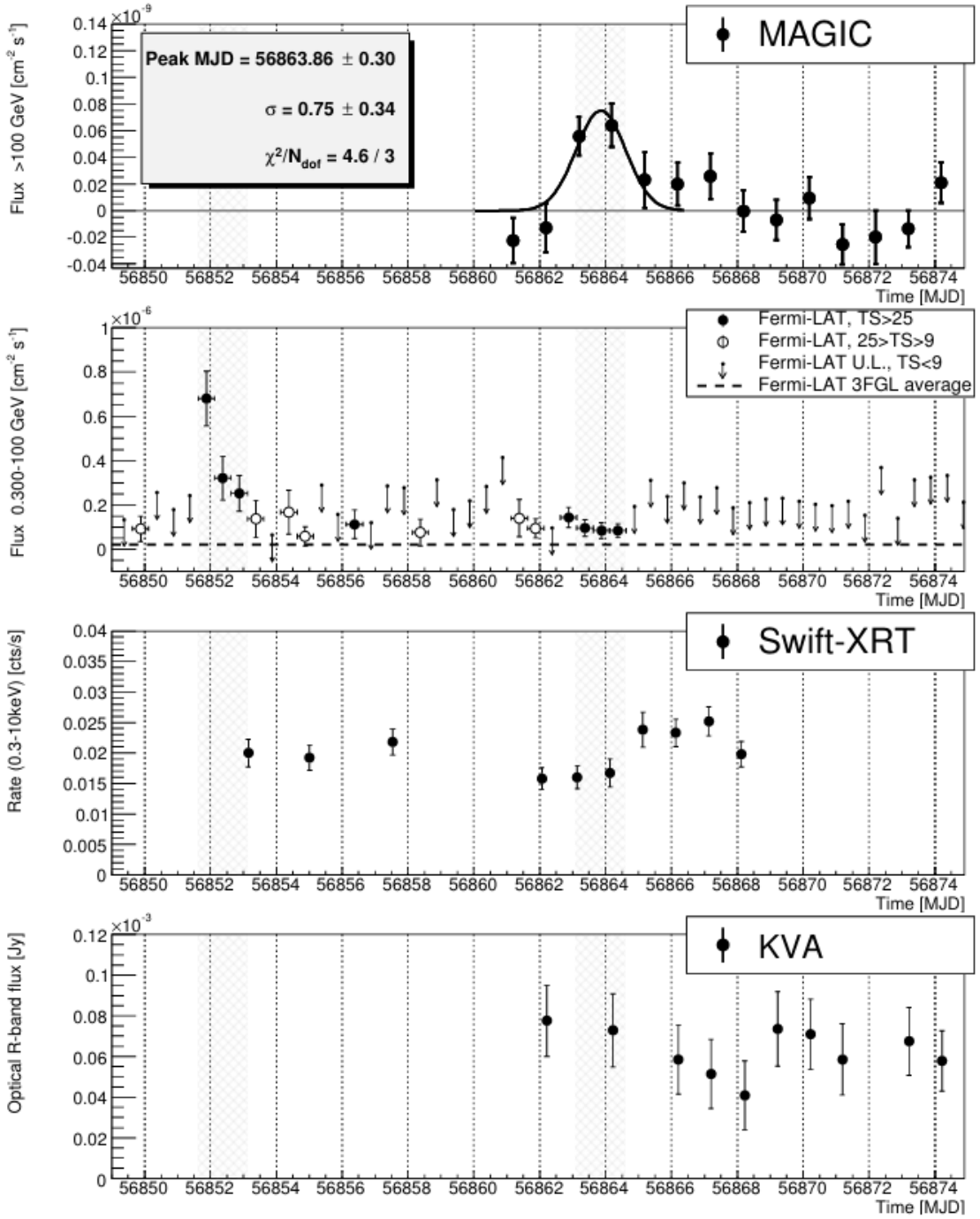

SED observed by MAGIC is represented by solid red circles and extends **from 65 to 175 GeV**.

EBL Deabsorption: After correcting (empty blue squares) using the EBL model from Domínguez et al. (2011), the intrinsic spectrum shows a **spectral index of 2.35** (slope of the line represents the SED)

Fermi-LAT comparison: The black diamonds show the Fermi-LAT spectrum from the same period, while the black dots represent the average emission of QSO B0218+357 as reported in the third catalog of Fermi-LAT sources.

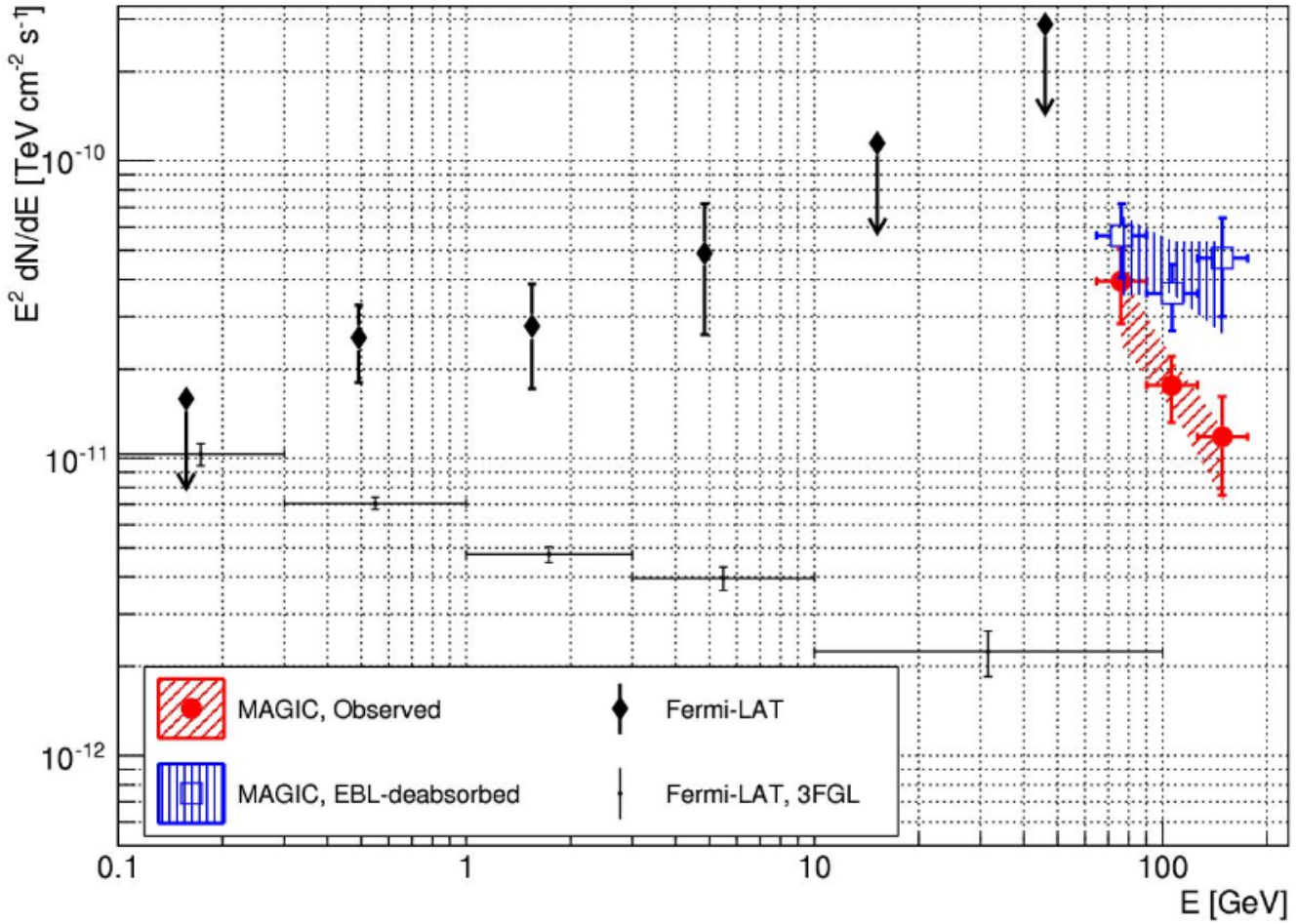

Fig. 3. Gamma-ray SED of QSO B0218+357 as observed during the two flaring nights, 2014 July 25 and 26, by MAGIC (red filled circles) and after deabsorption in EBL according to the Domínguez et al. (2011) model (blue open squares). The shaded regions show the 1 standard deviation of the power-law fit to the MAGIC data. Black diamonds show the *Fermi*-LAT spectrum from the same time period. Black points show the average emission of QSO B0218+357 in the 3FGL catalog (Acero et al. 2015).

LIGHT CURVE

- first follow the original alert + break + expected time of arrival of the delayed component.
- Photon Counting (PC) mode with count rates about 0.02 counts/s.
- Weak X-ray emitter and little variability-> observed emission is the sum of the two images of the source, with at least one of them affected by the hydrogen absorption.

Following the detection of the molecular absorption line in the A image, they include hydrogen absorption in the first component. If the same absorption is affecting both images the fit probability is worse.

Assumption: the absorption affects only the leading image

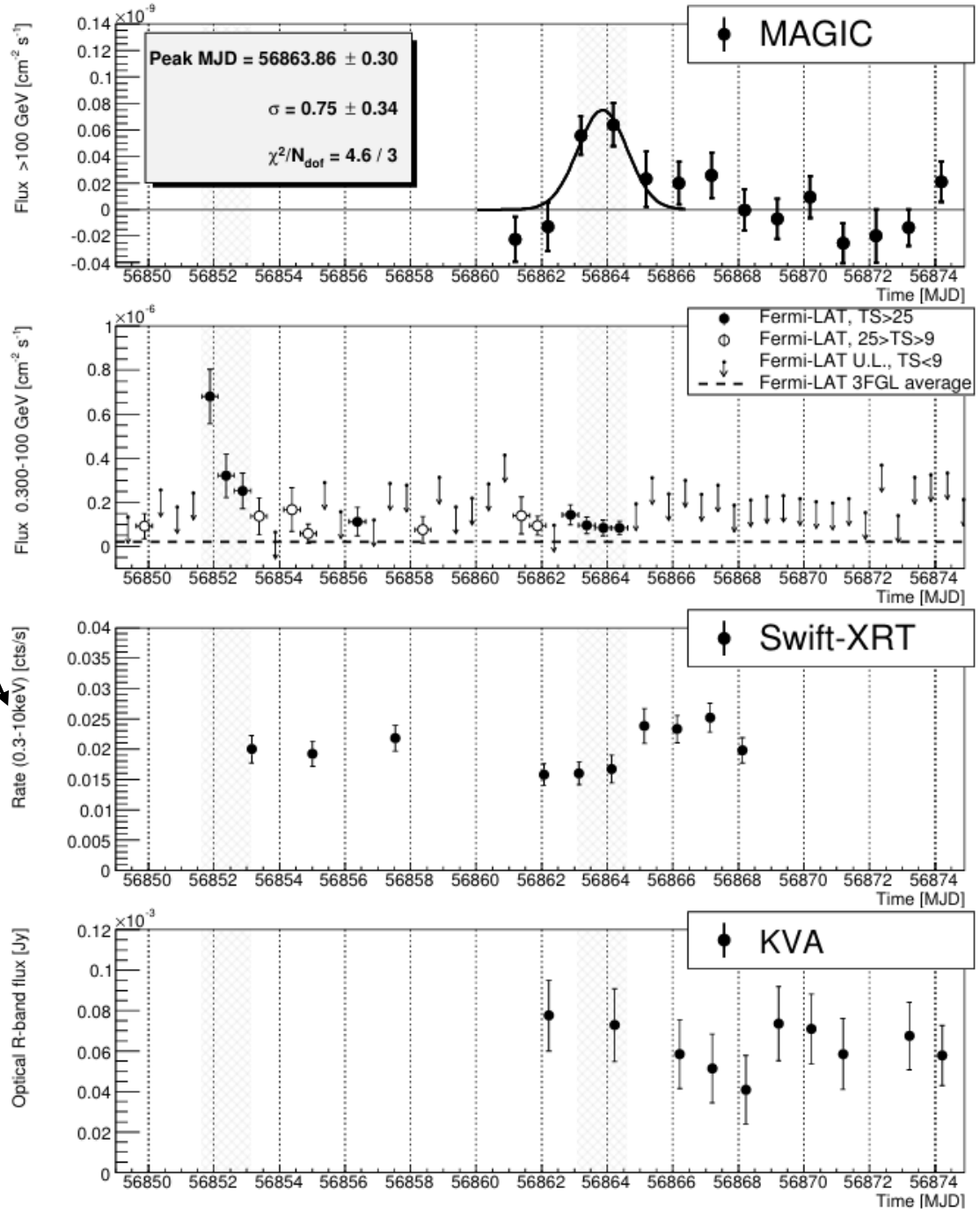

Observed energy counts in different energy ranges (keV)

Weak X-ray emitter and little variability-> observed emission is the sum of the two images of the source

The A image component is amplified and has additional absorption of hydrogen.
The B image component is intrinsically fainter but is not absorbed by the lensing galaxy.

The total model is composed of two power-law components, one for image A and one for image B, with the same spectral slope, but with different magnifications and hydrogen absorption affecting only the A image.

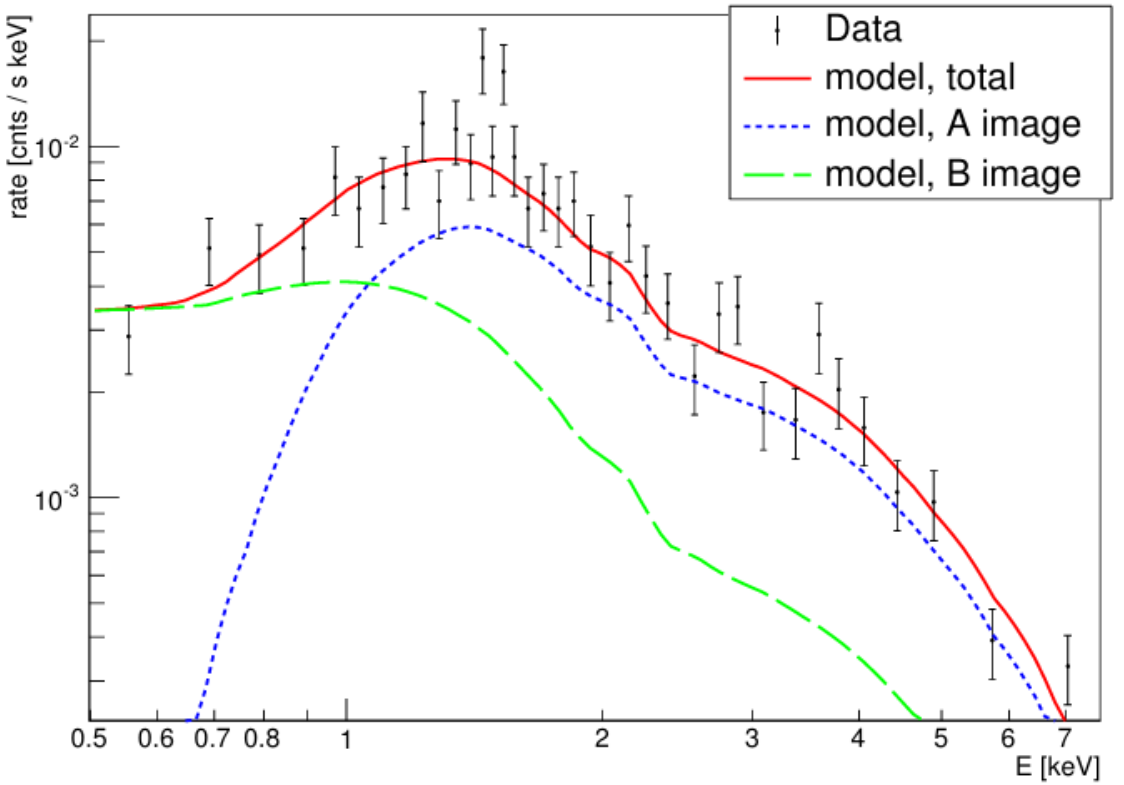

Fig. 4. Energy-binned counts observed by *Swift*-XRT from the direction of QSO B0218+357 (data points). The emission is modeled as a sum (solid red line) of two power-law components with the same spectral index. The first component (A image) is magnified by a factor 2.7 with an additional strong hydrogen absorption at the lens (dotted blue line). The second component (B image) is intrinsically weaker (magnification factor 0.7), but not absorbed at the lens (dashed green line).

LIGHT CURVE

- Faint (about 19 mag) -> error bars relatively large
- No significant variability was detected

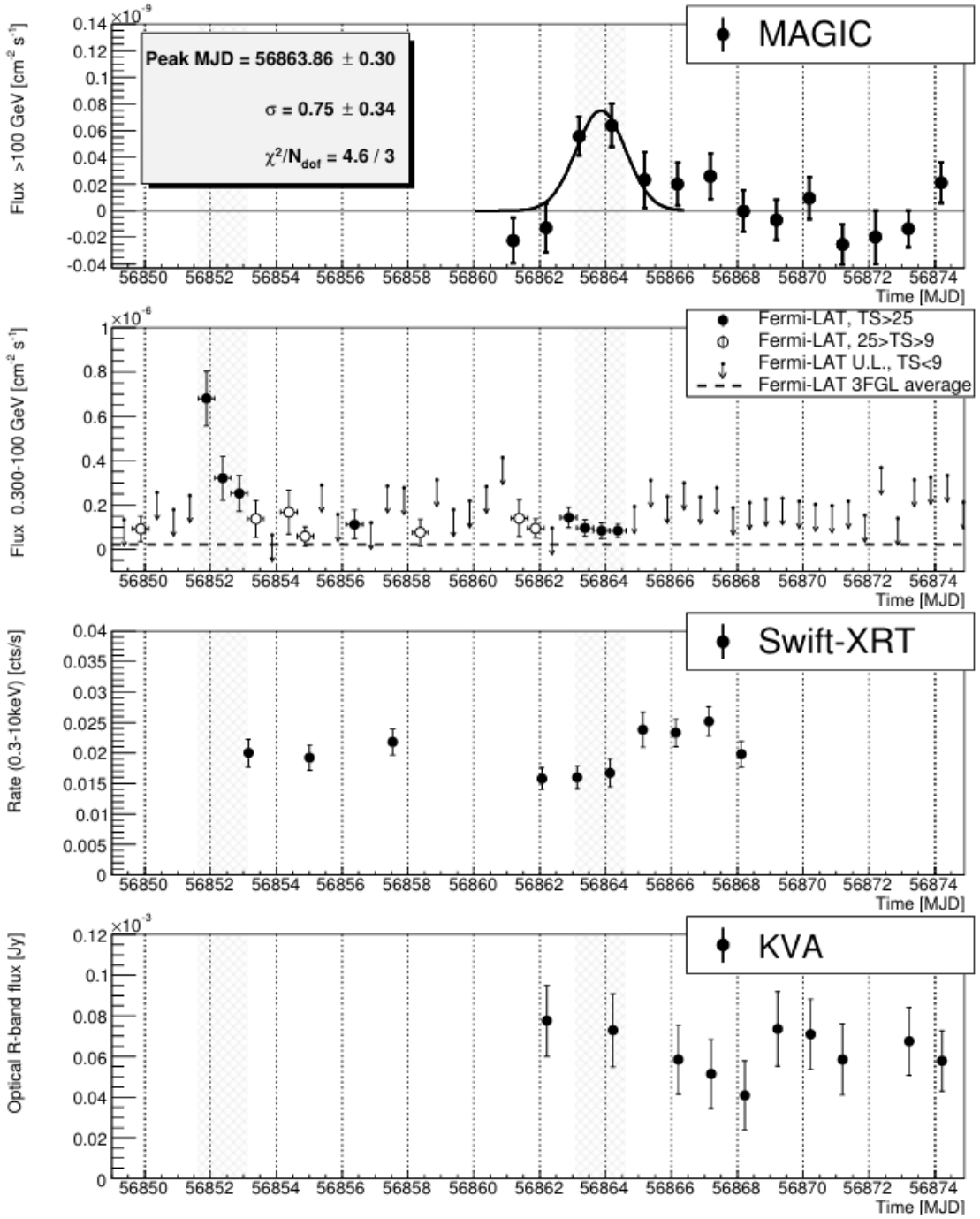

Broadband SED modeled with a two-zone model

red squares: reconstructed fluxes corrected for different magnifications in different energy ranges.
Green: Historical measurements
Dashed-dotted light blue line: accretion disk emission and its X-ray corona
Gray curves: emission from the region within the BLR
orange curves: emission from region beyond the BLR

Long dashed curves: synchrotron radiation
Dotted: the synchrotron-self-Compton emission
short dashed: external Compton emission

solid black line: sum of the non-thermal emission.

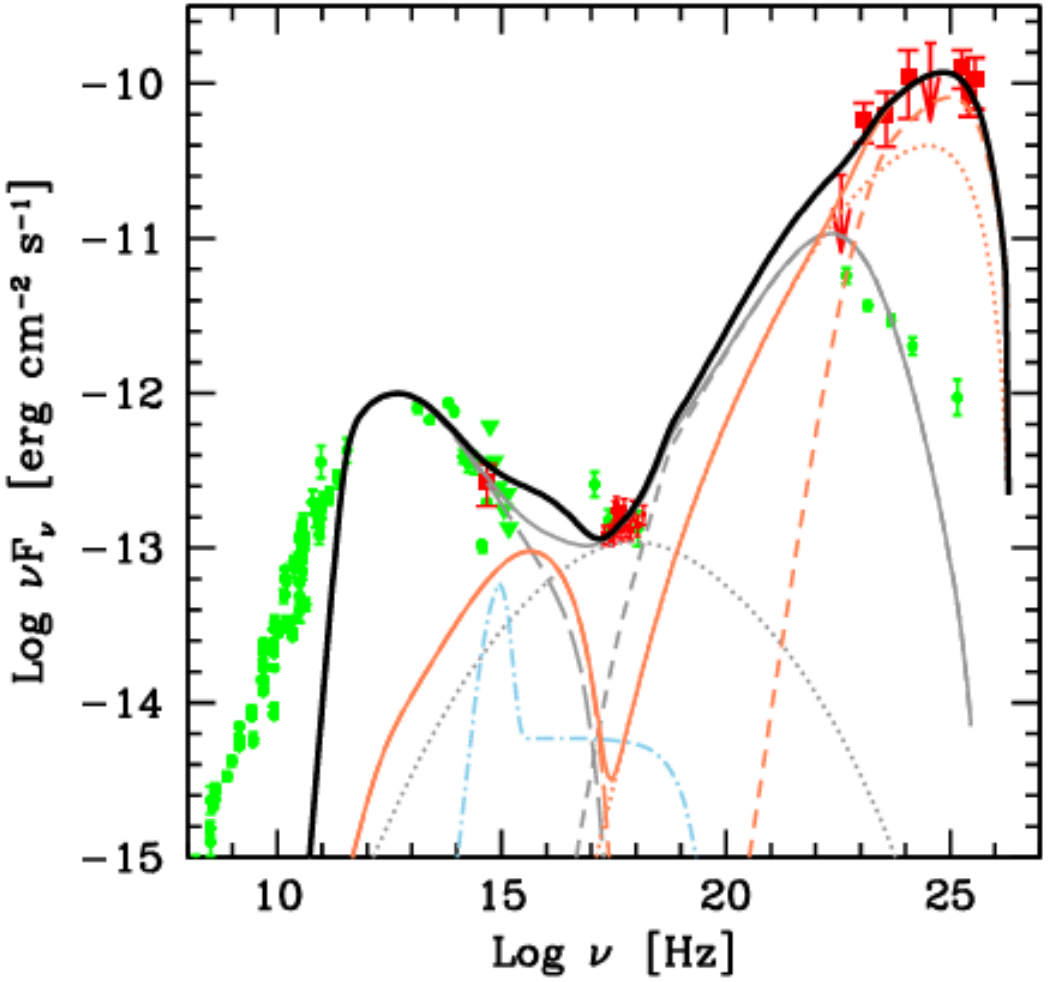

Broadband SED modeled with a two-zone model

Two peaks have a large separation in frequency and this cannot be easily explained in the framework of *one-zone leptonic models* (one would expect various emissions, such as radio and gamma, to be correlated and have close frequency peaks)

TWO-ZONE EXTERNAL COMPTON MODEL

- Two emission regions are moving along the jet
- Simplest assumption that the first emission region is located, as in the case of other FSRQs, inside the BLR
- Opacity condition forces the second emission region to be outside of the BLR

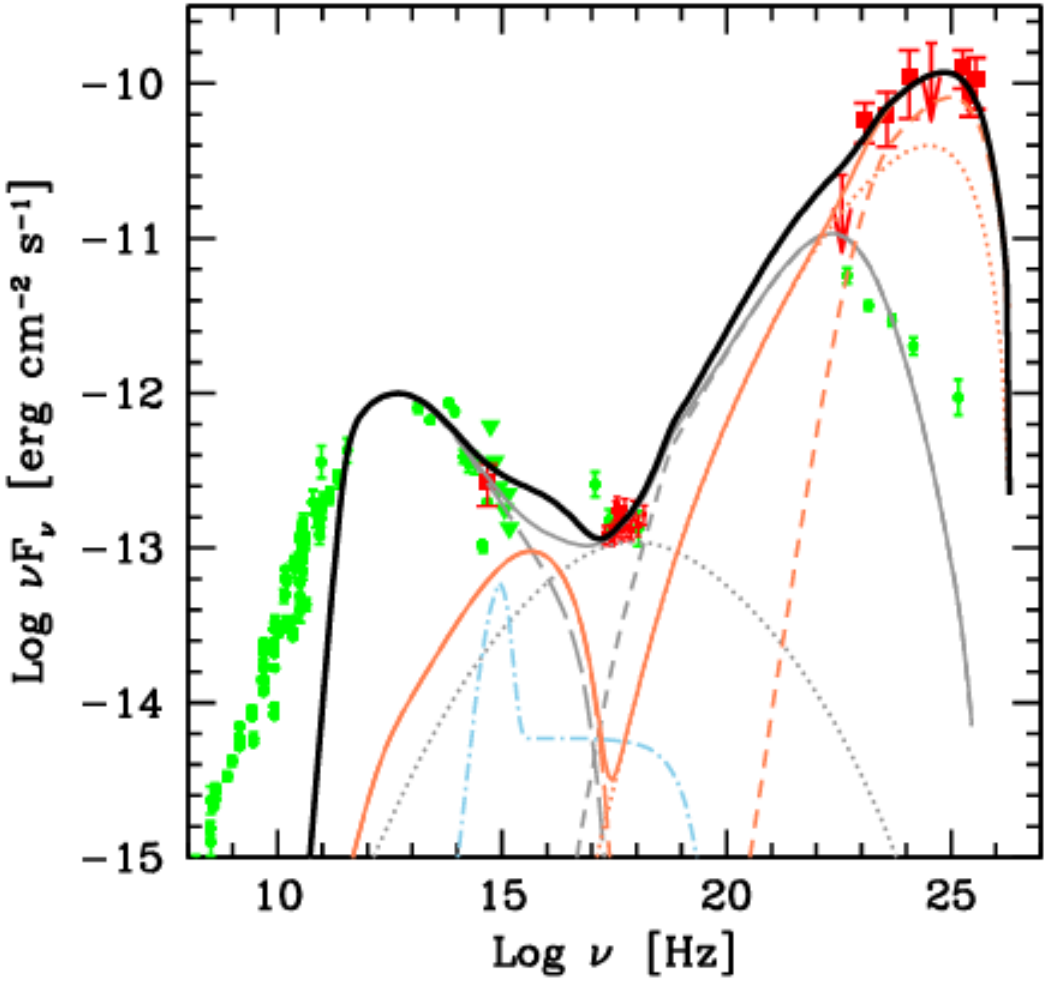

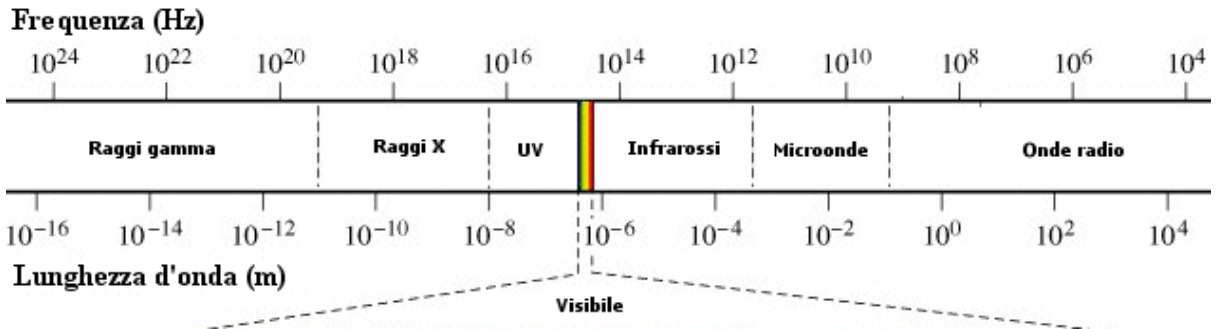

EBL absorption at z = 0.944

- Fermi-LAT and MAGIC data can be used to constrain the absorption of the EBL.
- The intrinsic spectral shapes are attenuated by EBL according to Domínguez et al. (2011)
- Spectral fit combining Fermi-LAT and MAGIC points using a set of possible spectral shapes

Probability of a SED fit as a function of the EBL scaling parameter α of the optical depth

The 1σ statistical uncertainty bounds of the α parameter can be obtained as the range of α in which the χ2 increases by 1 from the minimum value.

light scale is decreased (increased) by 15% in left (right) panel

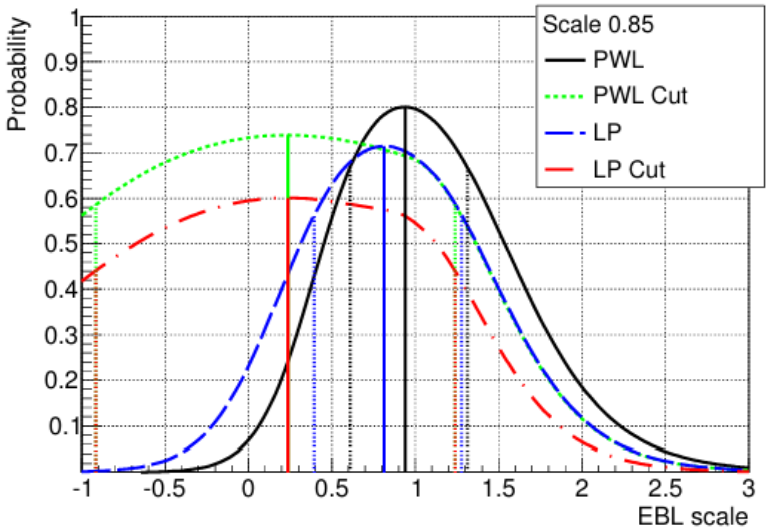

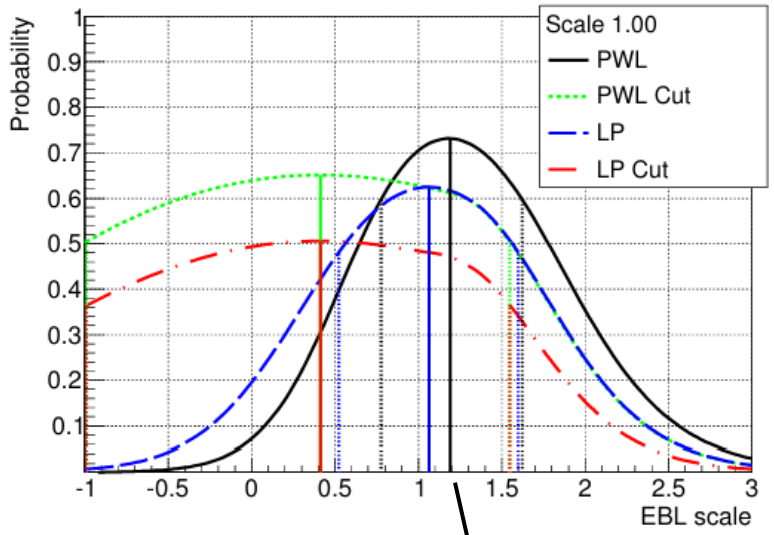

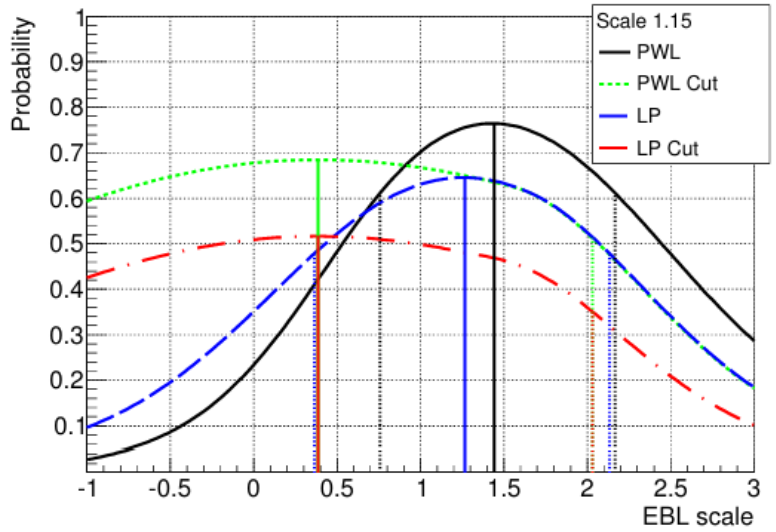

$$\text{PWL} : \mathrm{d}N/\mathrm{d}E = AE^{-\gamma},$$
$$\text{PWLCut} : \mathrm{d}N/\mathrm{d}E = AE^{-\gamma}\exp(-E/E_{cut}),$$
$$\text{LP} : \mathrm{d}N/\mathrm{d}E = AE^{-\gamma-b\log E},$$
$$\text{LPCut} : \mathrm{d}N/\mathrm{d}E = AE^{-\gamma-b\log E}\exp(-E/E_{\mathrm{cut}})$$
$$E_{\mathrm{cut}} > 0,\ b > 0$$

$$\alpha = 1.19 \pm 0.42_{\mathrm{stat}} \text{ at a redshift of } 0.944$$

Highest fit probability with the simple power-law spectral model (also with other EBL models)-> estimation of the EBL scaling parameter (consistent with all models considered)

All spectral shapes get a similar upper limit, it's not the same for the lower limit

RECAP

- Using the EBL model from Domínguez et al. (2011), the intrinsic spectral index in this energy range was found to be $2.35 \pm 0.75_{stat} \pm 0.20_{syst}$.
- The broad band emission of QSO B0218+357 is modeled in a framework of a two-zone external Compton model.
- The combined Fermi-LAT and MAGIC energy spectrum is consistent with the current EBL models

Thanks for the attention